0026-895X/91/0258-09$03.00/0

MOLECULAR PHARMACOLOGY, 39:258-266

Catabolism of 3′-Azido-3′-deoxythymidine in Hepatocytes and Liver Microsomes, with Evidence of Formation of 3′-Amino-3′-deoxythymidine, a Highly Toxic Catabolite for Human Bone Marrow Cells

ERIKA M. CRETTON, MENG-YU XIE, RAE J. BEVAN, NAGANNA M. GOUDGAON, RAYMOND F. SCHINAZI, and JEAN-PIERRE SOMMADOSSI

Department of Pharmacology, Center for AIDS Research, Comprehensive Cancer Center, Division of Clinical Pharmacology, University of Alabama at Birmingham, Birmingham, Alabama 35294 (E.M.C., M.-Y.X., R.J.B., J.-P.S.), and Veterans Affairs Medical Center and Laboratory of Biochemical Pharmacology, Department of Pediatrics, Emory University School of Medicine, Atlanta, Georgia 30033 (N.M.G., R.F.S.)

Received August 30, 1990; Accepted November 14, 1990

SUMMARY

Metabolic studies in humans have demonstrated that 3′-azido-3′-deoxythymidine (AZT) is primarily eliminated as its 5′-*O*-glucuronide (GAZT). However, no detailed cellular metabolic studies have been reported on the complete catabolic fate of AZT at the hepatic site. Because the liver is probably the major site of AZT catabolism, the metabolism and transmembrane distribution of AZT were evaluated in freshly isolated rat hepatocytes, a model for the study at the cellular level of biosynthetic, catabolic, and transport phenomena in the liver. Following exposure of cells to 10 μM [^{3}H]AZT, the predominant intracellular catabolite was GAZT, which reached a concentration of approximately 22 μM by 60 min. Additionally, under nonreducing conditions substantial levels of two previously unidentified AZT catabolites that were formed at the hepatic site and were distinct from any known anabolites or catabolites were also detected. These catabolites were identified as 3′-amino-3′-deoxythymidine (AMT) by fast atom bombardment mass spectrometry and 3′-amino-3′-deoxythymidine glucuronide (GAMT) through specific enzymatic hydrolysis. However, AMT was not a substrate for uridine 5′-diphosphoglucuronyltransferase and GAMT was found to be a reductive product of GAZT. Studies using rat and human liver microsomes demonstrated that the rate of formation of AMT and GAMT increased in the presence of NADPH, suggesting the involvement of a NADPH-dependent enzyme system. Studies using human hematopoietic progenitor cells demonstrated that AMT was 5- to 7-fold more toxic to human colony-forming units granulocyte-macrophage and burst-forming units erythroid than was AZT. This study provides the first detailed catabolic profile of AZT at the hepatic site and emphasizes the critical role that the liver plays in drug clearance. Formation of AMT, a highly toxic catabolite of AZT, raises a question regarding the role of AMT in the cytotoxic effects of AZT observed in patients.

AZT is currently the only drug clinically approved for the treatment of acquired immunodeficiency syndrome. Studies over the past years have demonstrated the importance of the intracellular anabolism of AZT to its phosphorylated metabolites and have clarified the role of this metabolism in both its antiviral and its cytotoxic effects in host cells (1–5). In contrast, detailed knowledge of the catabolic pathway is still limited, even though it has been suggested that approximately 80% of administered AZT in humans is primarily eliminated as a 5′-*O*-glucuronide (6, 7). Formation of GAZT has also been demonstrated in other species, such as rats, mice, and dogs (8), but at less than 5% of the administered AZT dose.

Recent studies by our group and others have reported the kinetic parameters of AZT glucuronidation in both rat and human liver microsomes. AZT exhibited a lower Michaelis-Menten constant (K_m) and a 5- to 6-fold higher catalytic efficiency with human UDPGT, when compared with rat UDPGT (9, 10). Although this may have a role in the quantitative metabolic differences observed *in vivo* between the two species (i.e., rats versus humans), other factors may also be involved, such as recirculation through the enterohepatic circulation, elimination in bile, or degradation by β-glucuronidase.

This work was supported by United States Public Health Service Grants AI-25784 and HL-42125 (J.-P.S.) and Grant AI-26055 and the Department of Veterans Affairs (R.F.S.). J.-P.S. is a recipient of a Junior Faculty Research Award from the American Cancer Society.

ABBREVIATIONS: AZT, 3′-azido-3′-deoxythymidine; GAZT, 3′-azido-3′-deoxy-5′-β-D-glucopyranuronosylthymidine; UDPGT, uridine 5′-diphosphoglucuronosyltransferase; AMT, 3′-amino-3′-deoxythymidine; GAMT, 3′-amino-3′-deoxy-5′-β-D-glucopyranuronosylthymidine; HPLC, high performance liquid chromatography; UDPGA, uridine 5′-diphosphoglucuronic acid; FAB, fast atom bombardment; MS, mass spectrometry; CFU-GM, colony-forming unit granulocyte-macrophage; BFU-E, burst-forming unit erythroid.

In that context, Mays *et al.* (11) have recently demonstrated that approximately 14% of administered AZT was recovered as GAZT in bile and urine of rats with exteriorized bile ducts.

Because the liver is probably the major site of AZT catabolism, an isolated rat hepatocyte system, a model for the study at the cellular level of biosynthetic, catabolic, and transport phenomena in the liver, was used to assess, for the first time, the catabolism of AZT using intact cells. This system permits analysis of drug-cell interactions, as well as eliminating complexities of studies with the intact liver or liver slices, such as alterations in blood flow, uncertainties about drug concentration at the cell membrane site due to large unstirred extracellular spaces, and contributions to drug transport and metabolism by other cell types in the liver (i.e., hepatic reticuloendothelial cells).

Using this approach, after exposure of cells to a clinically relevant concentration of 10 μM [^{3}H]AZT, rapid and extensive formation of GAZT was detected. Two previously unrecognized AZT catabolites that were formed by the hepatocytes were identified as AMT and GAMT. The previous findings of Prusoff and colleagues (12, 13) that AMT, a compound that was studied as a potential anticancer agent, was particularly cytotoxic to L1210 cells *in vitro*, prompted us to investigate whether this AZT catabolite may have a role in the myelosuppressive activities observed in patients after administration of AZT (14–16). Toxicity data obtained using human bone marrow clonogenic assays demonstrated that AMT was at least 5- to 7-fold more toxic for CFU-GM and BFU-E than was AZT. These data indicate the crucial role of the liver in the rapid elimination of AZT, which, in particular, led to the formation of a highly toxic catabolite, AMT. Hence, this organ plays an important role in determining the interval over which human immunodeficiency virus-infected cells are exposed to AZT *in vivo* and may amplify the toxic effects specific to AZT (1) by reducing this agent to AMT.

Materials and Methods

Chemicals

[5-^{3}H]AZT (3 mCi/mmol) and [5-^{3}H]AMT (1.7 mCi/mmol) were obtained from Moravek Biochemicals, Inc. (Brea, CA). [*carboxyl*-^{14}C] Inulin was purchased from DuPont Research Products (Wilmington, DE). [5-^{3}H]AZT and [5-^{3}H]AMT were 99% pure, as ascertained by the HPLC technique described below. [^{3}H]GAZT was isolated and purified by HPLC as previously described (9), and [^{3}H]GAZT purity was 99%, as assessed by HPLC. AZT was synthesized in our laboratory by the procedure of Lin and Prusoff (17) and had a purity of >99%, as assessed by HPLC. The structure of the compound was confirmed by proton NMR, ^{13}C NMR, and IR spectroscopy. Saccharo-1,4-β-lactone, β-NADPH (reduced form), UDPGA, alkaline phosphatase, venom phosphodiesterase I (type VI), and 0.2% ninhydrin in solution were purchased from Sigma Chemical Co. (St. Louis, MO). All other chemicals used were reagent grade.

Preparation of Hepatocyte Suspension and Incubation Conditions

Studies were performed utilizing rat hepatocytes in suspension, which were freshly isolated from Sprague-Dawley rats (180–200 g; Harlan Laboratories, Indianapolis, IN) by a modification of the method of Berry and Friend (18), which increases cell yield and viability as described previously (19). Cell viability, determined by trypan blue exclusion, was ≥90% in all experiments. Hepatocytes were suspended to a final cytocrit of 10% and were incubated at 37° in Krebs-Henseleit buffer, containing 0.25% (w/v) gelatin and 10 mM glucose, for intervals up to 2 hr. The pH was maintained at 7.4 by passage of warmed and humidified 95% O_2/5% CO_2 over the cell suspension. Experiments were initiated by the addition of [^{3}H]AZT (specific activity, 200 dpm/pmol) to achieve a final concentration of 10 μM. Times of incubation in the text represent the length of time between introduction of radiolabel into the cell suspension and starting of the microfuge. Portions of the cell suspension (0.5 ml) were layered onto 0.4 ml of inert silicon oil of density 1.2 (19), in 1.5-ml Eppendorf microfuge tubes. The tubes were immediately centrifuged at 15,000 × *g*, in an Eppendorf model 5314 microcentrifuge, for 30 sec, and the cell pellet was frozen in dry ice/acetone. Portions of the extracellular medium (50 μl) were then analyzed by HPLC, as described below, without further processing. After removal of the remaining extracellular medium and aspiration of the silicon layer, the frozen cell pellet was transferred to a plastic tube immersed in ice and was subjected to sonic oscillation in 1 ml of 2 mM potassium phosphate (pH 7.4), with a 300 probe sonicator (Artex, Farmingdale, NY), for 30 sec, to release intracellular ^{3}H. The sonicate was centrifuged at 15,000 × *g* at 4° in a Damon B-20A centrifuge, for 20 min, to pellet cellular debris. Fifty to 100 μl of the supernatant were then analyzed by HPLC (as described below). Usually, 50-μl portions of the extracellular and cell sonicate (after centrifugation) were analyzed to determine total ^{3}H in each compartment.

Analysis of Intracellular and Extracellular [^{3}H]AZT and Its Catabolites by HPLC

Fifty- to 100-μl aliquots of the intracellular or extracellular compartments were analyzed by HPLC using a Hewlett-Pachard model 1090 liquid chromatograph equipped with automatic injector, fixed wavelength spectrophotometer, and chromatographic terminal (Hewlett-Packard 85 B). Reverse phase chromatography was carried out using a Hypersil ODS 5-μm column (Jones Chromatography, Littleton, CO). Elution was performed at 1 ml/min with 25 mM phosphoric acid, adjusted to pH 7.2, and a 35-min linear gradient of acetonitrile from 0 to 30%, starting at the time of injection. Column temperature was maintained at 25° and absorbance was recorded at 254 nm. Eluent from the column was directed, via a low-dead volume connection line, into an LKB 2112 Redirac fraction collector (LKB Instruments, Rockville, MD), and timed fractions of 0.5 ml were collected into miniscintillation vials over 35 min. After addition of 5 ml of Budget-Solve scintillation fluor (Research Products International Corp., Mount Prospect, IL), radioactivity was measured using a Beckman 5801 liquid scintillation counter equipped with an automatic quench correction program. Under the aforementioned conditions, retention times of the unlabeled markers GAZT and AZT were 13–14 min and 21–22 min, respectively. The total radioactivity applied to the column was recovered for both extracellular and intracellular compartments in 35 min (95 ± 2% recovery, based upon 96 analyses).

Determination of Intracellular Water

Intracellular and extracellular water volumes were determined on unwashed pellets, using [^{14}C]inulin as an extracellular marker and gravimetric determination of wet and dry cell weights, as described previously (20). A portion of the hepatocyte suspension (6 ml) was incubated under the same conditions described above but was exposed to 0.4 μCi of [*carboxyl*-^{14}C]inulin for 10–15 min, to establish equilibrium between the extracellular and intracellular compartments. Five portions of the cell suspension (0.5 ml) were layered onto silicon oil and centrifuged at 15,000 × *g* for 30 sec. Determination of the radioactivity in the pellet provided a measure of the extracellular buffer solution that accompanies cells through the oil. This value was used to correct values for AZT and individual catabolites present in the cell pellet under these conditions. Five other samples were used to determine intracellular water volumes. These were placed in weighted Eppendorf microfuge tubes and centrifuged for 10 sec. Supernatants were used for determination of [^{14}C]inulin, and wet and dry weights of the pellets were obtained. The dried pellets were digested in 250 μl of 1 M KOH for 1 hr at 70°, cooled, neutralized with 1 M HCl, and mixed with 5 ml

of Budget-Solve (Research Products), and radioactivity was measured. Intracellular water was the difference between the wet and dry weights of the cell pellet, minus the [^{14}C] inulin volume. Intracellular and extracellular values were 20.6 ± 3.9 and 7.5 ± 1.3 μl (five determinations), respectively.

Isolation and Preliminary Identification of AZT Catabolites

Incubation with alkaline phosphatase and 5′-phosphodiesterase. A total of approximately 5000 dpm of X_1 or X_2 was isolated by HPLC and incubated with 0.31 units of alkaline phosphatase, in 50 mM potassium phosphate buffer, 1 mM $ZnSO_4$ (pH 6.5), for 4 hr at 37° (total volume, 150 μl). Reaction was terminated by addition of 30 μl of cold 50% trichloracetic acid. After 30 min at 4°, samples were centrifuged for 1 min at 15,000 × *g*, in an Eppendorf model 5314 microcentrifuge. The supernatant was neutralized with 60 μl of 5 M potassium bicarbonate, and an aliquot was analyzed by HPLC, as described above. Control incubations were performed with heat-inactivated enzyme. Similar incubation conditions as described above were used for 5′-phosphodiesterase hydrolysis, except that 0.048 unit/ml (2 mg/ml) levels of that enzyme were present.

Ninhydrin test. Preliminary identification of X_1 and X_2 was performed using a ninhydrin dye, which produces a colored product when it reacts with a free amino group. Samples of X_1 and X_2 were isolated from intracellular medium by HPLC. The fractions corresponding to each compound were separately pooled and lyophilized. The dry residues were then dissolved in 2.0 ml of water, passed through a 0.45-μm Acro LC 13 filter (Gelman Sciences, Ann Arbor, MI), and then applied to a Sep-Pak C_{18} cartridge (Waters Associates, Inc., Milford, MA). The cartridge was then washed four times with 5 ml of water, and 80–90% of the radioactivity initially applied to the Sep-Pak was recovered. Portions (20 ml) were pooled and lyophilized. The dry residues corresponding to X_1 and X_2 were redissolved in 1.0 ml of water, and 250-μl portions were chromatographed, as described above, to ensure purity and complete separation of these two metabolites. Approximately 10,000 dpm of purified X_1 and X_2 were then spotted, together with authentic AZT and GAZT standards, on a silica gel GF 500-μm thin layer chromatography plate; aspartic acid was used as a positive control. The plate was then developed in a mixture of ethyl acetate/acetic acid (10:1) for approximately 2 hr, air dried, and sprayed with a 0.2% ninhydrin solution in ethanol.

Formation of X_1 and X_2 in human and rat liver microsomes. Studies were performed utilizing human and rat liver microsomes, isolated from transplant organ donors and Sprague-Dawley rats, respectively, as previously described (9). Protein content was determined by the method of Lowry *et al.* (21). All assay mixtures contained 0.04% (v/v) Triton X-100, 50 mM $MgCl_2$, 3 mg/ml microsomal proteins, 5 mM saccharo-1,4-β-lactone to inhibit β-glucuronidase that may be present, and 5 mM [^{3}H]AZT (0.4 mCi/mmol), in a final volume of 0.5 ml. Reactions were initiated by addition of either (i) no cofactors, (ii) 6 mM NADPH alone, (iii) 6 mM NADPH and 5 mM UDPGA, or (iv) 5 mM UDPGA alone. All samples were incubated at 37° for 45 min. Control incubations were performed with boiled microsomal extracts, and experiments were carried out in duplicate under conditions leading to linear reaction rates with time and protein concentration. Incubations were terminated by boiling for 30 sec, and proteins were removed by centrifugation at 15,000 × *g* for 4 min, in an Eppendorf model 5314 microcentrifuge. Fifty- to 100-μl aliquots were analyzed by the liquid chromatographic methodology described above. In a similar fashion, approximately 20,000 dpm of GAZT were incubated at 37° for 1 hr with 6 mM NADPH, in the presence of 3.0 mg/ml rat microsomal protein, in a final volume of 1 ml. Control incubations were performed without coenzyme. Fifty- to 100-μl aliquots were then analyzed by HPLC, and a subsequent assay was performed with 10,000 units of β-glucuronidase in 0.2 M sodium acetate, pH 4.5, incubated at 37° overnight.

FAB-MS analysis. The identity of the X_2 chromatographic peak was confirmed by FAB-MS. The FAB mass spectrum of the compound suspended in glycerol was obtained using a Varian MAT 311 A (San Jose, CA), modified by AMD Intectra GmbH (Beckeln, Germany). The mass spectrometer was operated at an accelerating voltage of 5 kV and a resolution of 1000 (10% valley definition). The FAB gun was a FAB 11N (Ion Tech Ltd., Middlesex, England) operating at 8 kV and 1 mA current. Xenon was used as the bombardment gas.

Chemical synthesis of AMT standard. AZT (534 mg, 2 mmol) and triphenylphosphine (790 mg, 3 mmol) were dissolved in pyridine (6 ml), and the reaction solution was stirred at room temperature for 1 hr. Concentrated ammonium hydroxide (1.6 ml) was then added, and the solution was stirred for an additional 2 hr. Pyridine was removed under reduced pressure, water (10 ml) was added, and triphenylphosphine and triphenylphosphine oxide were removed by filtration. The filtrate was extracted with ether to remove residual triphenylphosphine and then concentrated to dryness. Recrystallization of the solid residue from ethanol afforded 320 mg (66%) of AMT (m.p. 158–160°). The chromatographic properties, FAB MS analysis, and proton NMR spectrum were identical to those of an authentic standard kindly provided by Dr. W. H. Prusoff, Yale University (New Haven, CT), and described previously (17).

Clonogenic Assays for Drug Cytoxicity

Human bone marrow cells were collected by aspiration from the posterior iliac crest of normal healthy volunteers, according to a protocol approved by the Institutional Review Board Committee at the University of Alabama at Birmingham. Cells were treated with heparin, and the mononuclear population was separated by Ficoll-Hypaque gradient centrifugation, as described previously (22). Cells were washed twice in Hanks' balanced salt solution and counted with a hemacytometer, and their viabilities were >98%, as assessed by trypan blue exclusion. The culture assays were performed by using a bilayer soft agar or methylcellulose method (22). McCoy's 5A nutrient medium supplemented with 15% dialyzed fetal bovine serum (heat inactivated at 56° for 30 min) (GIBCO Laboratories, Grand Island, NY) was used in all experiments. This medium was devoid of thymidine and uridine. Human recombinant granulocyte/macrophage colony-stimulating factor (50 units/ml; Genzyme, Boston, MA) or erythropoietin (1 units/ml; Connaught, Swiftwater, PA) was used as colony-stimulating factor. After 14–18 days of incubation at 37° in a humidified atmosphere of 5% CO_2 in air, colonies (≥50 cells) were counted by using an inverted microscope. The clonogenic efficiency was between 0.1 and 0.2% in all experiments.

Results

HPLC Analysis of AZT and Its Catabolites after Incubation of Hepatocytes with [^{3}H]AZT

Fig. 1 represents the HPLC chromatogram of intracellular ^{3}H 30 min after incubation of hepatocytes with 10 μM [^{3}H] AZT. In addition to GAZT and AZT, two unknown peaks, labeled X_1 and X_2, were detected. These derivatives did not correspond to any known anabolite of AZT. Correspondence was ruled out due to different retention times observed with AZT 5′-phosphorylated derivatives and the resistance of X_1 and X_2 to both alkaline phosphatase and 5′-phosphodiesterase hydrolysis.

Identification of AZT Catabolites

Ninhydrin test. The nynhidrin test (see Materials and Methods) was positive with both unknown chromatographic peaks (X_1 and X_2), indicating that both AZT catabolites, X_1 and X_2, contain a free amino group. In contrast, as expected, the reaction was negative with AZT and GAZT standards, consistent with the fact that neither compound has a free amino group and that the azido moiety does not react with ninhydrin.

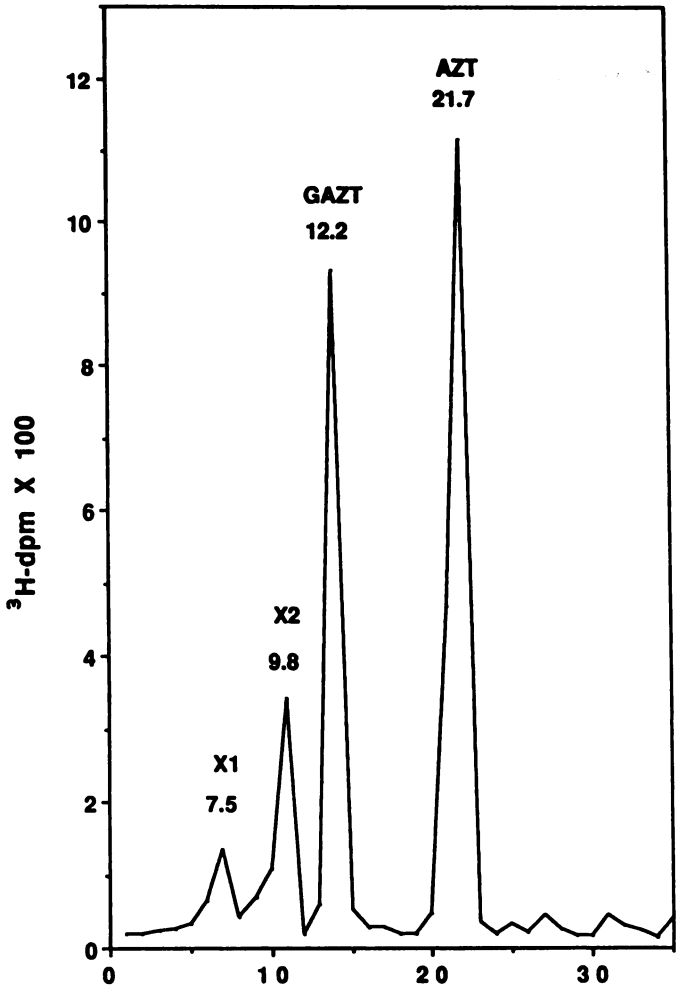

Fig. 1. HPLC profile of intracellular AZT and its catabolites X_1, X_2, and GAZT in freshly isolated rat hepatocytes 30 min after exposure to 10 μM [^{3}H]AZT. AZT and catabolites were resolved on an Hypersil ODS column by using 25 mM phosphoric acid (pH 7.2) and a 35-min linear acetonitrile gradient. UV absorbance was monitored at 254 nm.

Liver microsome assays. Table 1 summarizes the data obtained when microsomes isolated from either human or rat liver were incubated with 5 mM AZT and (i) no NADPH or UDPGA, (ii) NADPH alone, (iii) NADPH and UDPGA, or (iv) UDPGA alone (see Materials and Methods). In experiments that contained NADPH, X_2 was the major AZT catabolite, with a rate of formation of 98.0 and 20.9 × 10^{-4} μM/min/mg of protein, using human and rat microsomes, respectively. This rate of X_2 formation was enhanced approximately 20-fold in the presence of NADPH, as compared with condition iii, which lacked this cofactor. In contrast, UDPGA had no influence on the rate of formation of X_1 and X_2. X_1 formation was slightly enhanced by NADPH in rat microsomes. However, no substantial differences were observed when human microsomes were used. As expected, GAZT formation was dependent on UDPGA concentrations. Low levels of GAZT were also detected in the incubations containing only NADPH, probably due to the presence of residual endogenous UDPGA. Of note, the rate of formation of AZT catabolites was higher in human microsomes,

TABLE 1

Rate of formation of AZT catabolites in human and rat liver microsomes in the presence of NADPH, NADPH and UDPGA, or UDPGA, as described in Materials and Methods

Values are mean ± standard deviation of three experiments performed in duplicate.

Catabolite	Rate of formation			
	Control	NADPH	NADPH + UDPGA	UDPGA
	(μM/min/mg of protein) × 10^{-4}			
Human microsomes				
X_1	4.0 ± 0.5	5.0 ± 0.9	4.9 ± 1.4	4.3 ± 1.0
X_2	4.8 ± 1.1	98.0 ± 12.9	94.0 ± 8.6	5.3 ± 1.4
GAZT	3.0 ± 1.0	4.2 ± 0.5	100.0 ± 8.5	93.0 ± 10.6
Rat microsomes				
X_1	NA[a]	1.4 ± 0.2	1.0 ± 0.1	0.3 ± 0.1
X_2	NA	20.9 ± 5.5	17.0 ± 4.3	1.2 ± 0.4
GAZT	NA	0.6 ± 0.2	31.3 ± 1.5	42.7 ± 1.1

[a] NA, not available.

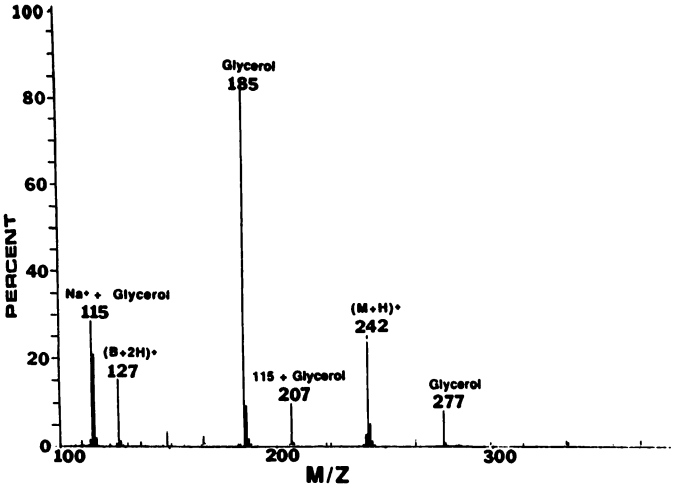

Fig. 2. FAB mass spectrum of X_2 formed in freshly isolated rat hepatocytes.

as compared with rat microsomes. These data rule out a potential chemical degradation or hydrolysis of AZT to X_1 and X_2 and suggest that the formation of X_2, and possibly X_1, involves an NADPH-dependent enzyme system.

FAB-MS analysis. The unknown chromatographic peak corresponding to X_2 was then evaluated by FAB MS analysis, as described in Materials and Methods. The FAB mass spectrum (Fig. 2) demonstrated a single positive molecular ion, $(M-H)^+$, at m/z 242 (25%). The molecular weight of this catabolite (241) and breakdown pattern was consistent with that of AMT. Other diagnostic ions that were present included the thymine base plus two protons at m/z 127 (15%). An identical FAB mass spectrum was obtained from an authentic chemically synthesized AMT standard.

Identification of X_1. Because sufficient X_1 could not be isolated from cells or incubation medium to allow detailed chemical characterization, enzymatic reactions were performed to identify this AZT catabolite and its route of formation. Fig. 3 represents the HPLC radiochromatogram of extracts of microsomes incubated with purified [^{3}H]GAZT in the absence (Fig. 3A) or presence (Fig. 3B) of 6 mM NADPH, as described in Materials and Methods. Addition of NADPH resulted in the detection of a radiolabeled peak with a retention time of 7–8 min, which coeluted with the catabolite fraction X_1 that was isolated from intracellular samples as described in Materials

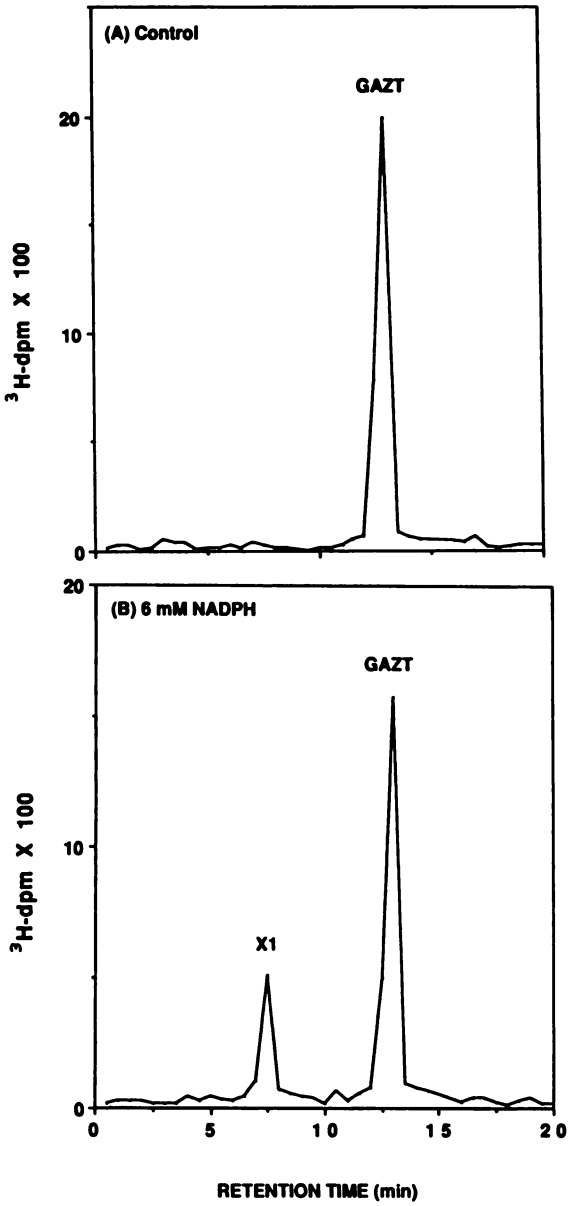

Fig. 3. HPLC radiochromatogram of GAZT following a 1-hr incubation with rat microsomes in the absence (A) and the presence (B) of 6 mM NADPH. Data are representative of three different experiments with duplicate incubations.

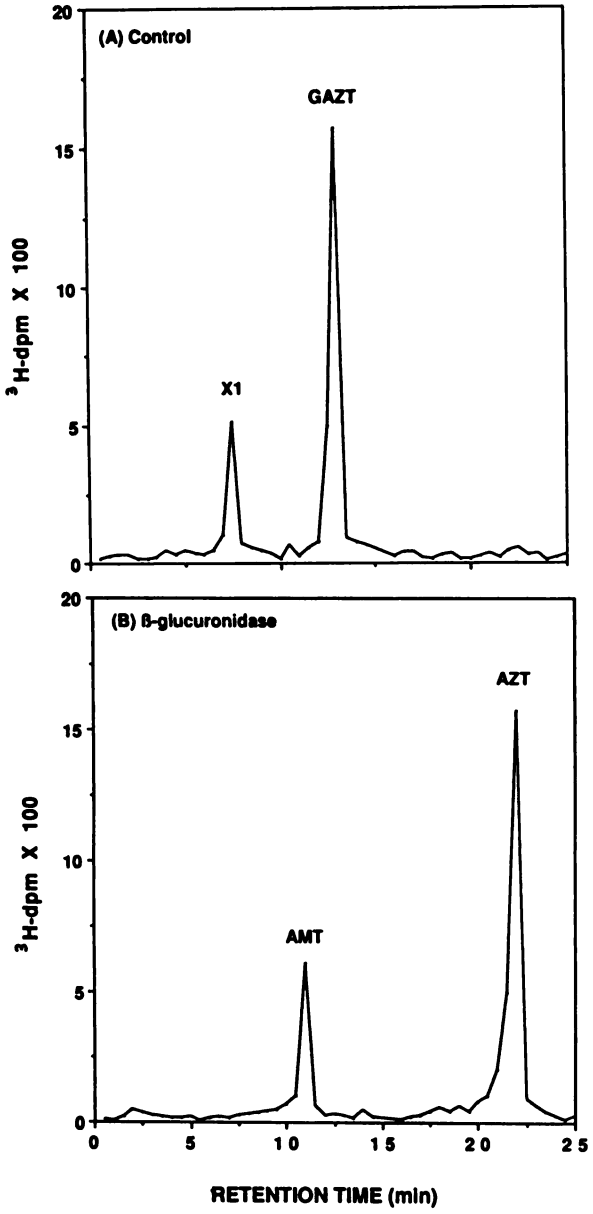

Fig. 4. HPLC radiochromatogram of GAZT and X_1 following incubation in the presence of boiled enzyme (A) and β-glucuronidase (B). Data are representative of three different experiments with duplicate incubations.

and Methods. This catabolite (X_1) was subsequently identified as a glucuronide of AMT through specific enzymatic hydrolysis by β-glucuronidase. Fig. 4B demonstrates that, in the presence of β-glucuronidase, the two chromatographic peaks detected in microsome extracts incubated with NADPH (Fig. 3B) were completely converted to radioactive peaks that coeluted with authentic AMT and AZT standards. In the presence of boiled enzyme (Fig. 4A), no significant radioactivity was found in the AMT and AZT regions of the radiochromatogram, indicating that conversion of X_1 to AMT and of GAZT to AZT is suppressed. Conversion of X_1 to AMT by β-glucuronidase was also demonstrated when purified X_1 from cell extracts was studied (data not shown). In additional studies, rat and human microsomes were exposed to 5 mM [^{3}H]AMT (0.4 mCi/mmol) in the presence of 5 mM UDPGA, and freshly isolated rat hepatocytes were incubated with 10 μM [^{3}H]AMT. In all experiments, GAMT was not found, indicating that AMT is not a substrate for UDPGT and that GAMT is exclusively formed from GAZT.

Time Course of Appearance of Intracellular AZT and Its Catabolites

The time course of appearance of unchanged AZT, GAZT, AMT, and GAMT in the intracellular medium is shown in Fig. 5. Unmetabolized AZT was detected at all time points over the 2-hr exposure within the hepatocytes. Intracellular AZT levels equaled those of the extracellular compartment, consistent with the demonstration that AZT crosses biological membranes by passive diffusion (23). The predominant catabolite in the intracellular medium was GAZT, which reached a steady state level of 22.3 ± 4.3 μM by 60 min; this level was maintained for the remaining 1 hr of the experiment. Within 5 min after the initial exposure of the hepatocyte suspension to [^{3}H]AZT, intracellular GAMT and AMT could also be detected. By 30 min, AMT

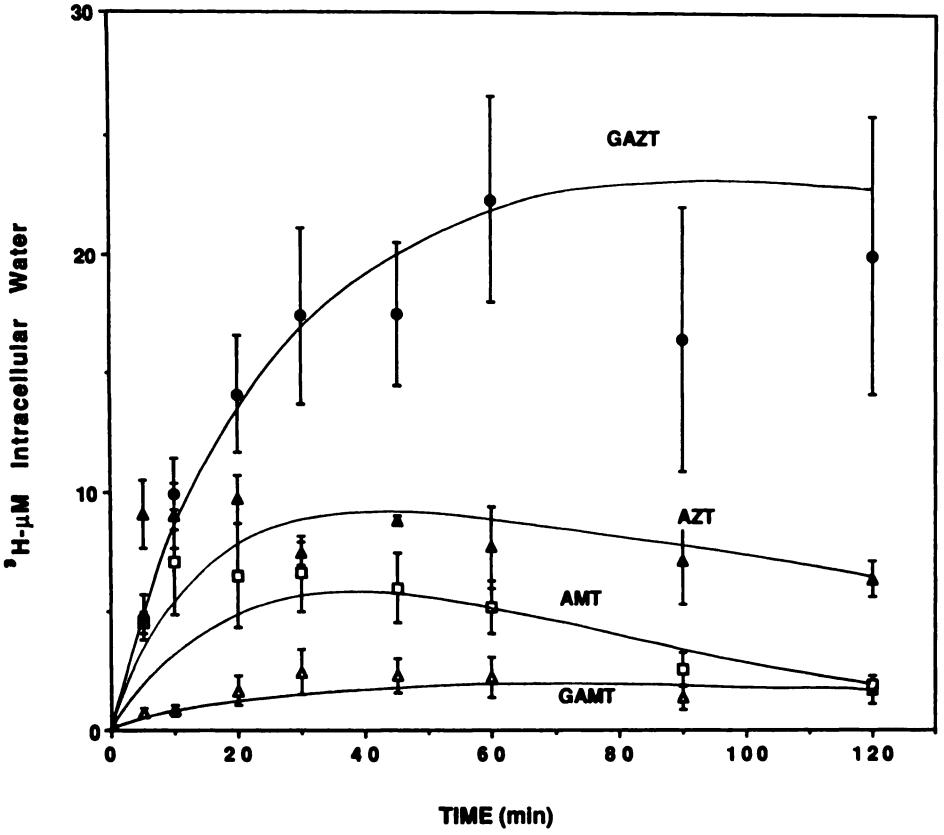

Fig. 5. Time course of appearance of unchanged AZT (▲), GAZT (●), AMT (□), and GAMT (△) in the intracellular water after exposure of cells to 10 μM [^{3}H]AZT. At the indicated times, portions of cell suspension were separated by centrifugation and extracted, and total intracellular ^{3}H was analyzed by HPLC. Corrections were made for extracellular AZT and its catabolites that accompany cells through the oil. All data presented represent the mean of six experiments ± standard error.

reached its peak intracellular concentration of 6.6 ± 1.6 μM, which subsequently declined to a level of 1.9 ± 0.3 μM by 2 hr. GAMT reached a steady state level of 2.2 ± 0.9 μM within the hepatocytes by 30 min, which was maintained for the remaining 1.5 hr of the experiment.

Analysis of the Time Course of Disappearance of Extracellular AZT and Appearance of Extracellular Catabolites

Analysis of extracellular AZT and its catabolites over 5 min to 2 hr after exposure of hepatocytes to [^{3}H]AZT is illustrated in Fig. 6. The extracellular level of AZT declined to one half of the initial level over 2 hr. As the level of extracellular AZT decreased, catabolites of AZT that were synthesized within the cells appeared in the extracellular compartment, with the exception of GAMT. Although this catabolite was not detected, a possible explanation for this observation is that GAMT levels were below the limit of sensitivity of 0.01 μM. Extracellular GAZT increased to a level of 4.0 ± 0.3 μM by 2 hr, although a maximum steady state level had not yet been reached. AMT also appeared rapidly in the medium, reaching a maximum steady state level of 0.18 ± 0.06 μM at approximately 30 min, and gradually declined. Results similar to those described above were obtained for both intracellular and extracellular compartments when hepatocytes were exposed to 10 μM [^{14}C]AZT (data not shown).

Toxicity of AZT and AMT for Normal Human Hematopoietic Progenitor Cells *In Vitro*

AZT was toxic to both human CFU-GM and BFU-E in a dose-dependent manner (Table 2), with a 50% inhibitory concentration of AZT for either CFU-GM or BFU-E being in the same range as that previously reported (22, 24). Consistent inhibition of CFU-GM and BFU-E occured at an AMT concentration of 0.4 ± 0.2 and 0.09 ± 0.05 μM, respectively. This toxicity was 5- to 7-fold higher than that of AZT, using cells from similar donors. As observed with other nucleoside analogs (25), BFU-E were more sensitive to AMT than were CFU-GM.

Discussion

These studies provide the first detailed analysis of the formation of AZT catabolites and their disposition in hepatic cells using a freshly isolated rat hepatocyte system. The results are summarized in Fig. 7, which demonstrates catabolic pathways of AZT in the hepatocyte. The major catabolic reaction is the conjugation of AZT with UDPGA, by UDPGT, resulting in a 5′-*O*-glucuronide. Initial studies in the rat indicated that this species excretes less than 5% of the administered AZT dose as this glucuronide (8), suggesting that AZT is not extensively glucuronidated in rats. Furthermore, we and others have suggested that AZT is not an efficient substrate for rat as compared with human UDPGT, using *in vitro* liver microsome systems (9, 10). In contrast, using intact isolated rat hepatocytes, GAZT was shown to be the major constituent of intracellular radioactivity after incubation of the hepatocytes with 10 μM [^{3}H] AZT. Extracellular GAZT levels increased steadily and maintained a 5-fold transmembrane gradient, suggesting that this catabolite exits from cells very slowly, relative to the rate at which it is synthesized. This poor permeability of GAZT may be due to the large carbohydrate moiety on this molecule and/or the ionization of GAZT in the intracellular compartment under the conditions of the experiment. The second catabolic pathway of AZT involves the reduction of the azide moiety, to

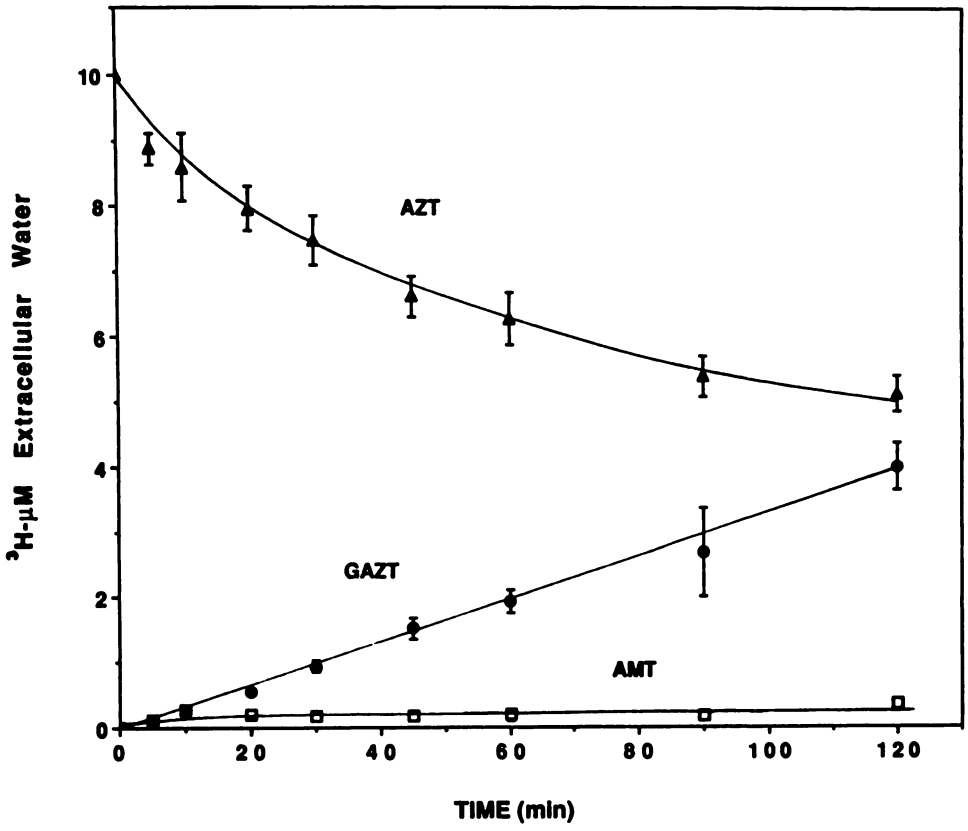

Fig. 6. Analysis of extracellular AZT (▲) and its catabolites GAZT (●) and AMT (□) after exposure of hepatocytes to 10 µM [^{3}H]AZT. At the indicated times, portions of the cell suspension were separated by centrifugation, and the total ^{3}H was assayed by HPLC. All data presented represent the mean of six experiments ± standard error.

TABLE 2

Effects of AZT and AMT on human myeloid (CFU-GM) and erythroid (BFU-E) progenitor cells, as assessed by clonogenic assays

Data represent mean values ± standard deviations of three separate experiments, with cells from different donors, performed in triplicate.

Treatment	Concentration	Cell growth		IC_{50}	
		CFU-GM	BFU-E	CFU-GM	BFU-E
	µM	% of control		µM	
AZT	0.1	78.3 ± 4.7	62.6 ± 10.2		
	1	61.4 ± 9.5	45.3 ± 4.6		
	10	38.3 ± 4.6	31.5 ± 5.1	1.9 ± 1.2	0.6 ± 0.5
	100	1.1 ± 1.9	5.3 ± 5.9		
AMT	0.1	65.0 ± 4.5	49.9 ± 4.6	0.4 ± 0.2	0.09 ± 0.05
	1	42.5 ± 6.2	22.5 ± 1.6		
	10	14.4 ± 4.0	0		
	100	0	0		

yield AMT, by a NADPH-dependent enzyme system. Handlon *et al.* (26) recently demonstrated the ability of thiols, such as dithiothreitol, to reduce AZT to a single product identified as AMT. The possibility that the reduction of AZT to AMT determined under the conditions of the present study is the result of a nonenzymatic reduction (i.e., by reducing agents) is remote, because samples (during either incubation of cells, processing of intracellular and extracellular samples, or HPLC analysis) did not come in contact with reducing agents at any time. Furthermore, when rat and human liver microsomes were exposed to AZT in the presence of NADPH, the rate of AMT formation increased approximately 20-fold, indicating that the formation of this catabolite is mediated by an enzymatic microsomal system that is NADPH dependent. Detailed characterization of this enzymatic step at the hepatic site is being pursued, and this reaction may involve a cytochrome P-450 reductase that has been previously shown to reduce the azide moiety of the antitumor agent metaazidopyrimethamine (27). Following incubation of the hepatocytes with 10 µM [^{3}H]AZT, intracellular AMT levels were considerably higher than extracellular levels, suggesting that AMT is slowly transported out of the cell, consistent with the high degree of polarity of this compound. Recently, De Miranda *et al.* (28) suggested formation of AMT by the intestinal microflora, as evidenced by its detection in rat feces. The AMT identity was suggested by comparison of the HPLC retention time of the biologically found AZT catabolite with that of an authentical chemically synthesized standard, but final proof of AMT identity by chemical analyses such as FAB-MS or proton NMR was not reported. In two recent studies on the transport and metabolism of AZT by the human placenta (29, 30) an unknown polar metabolite was detected under chromatographic conditions similar to those used by our group. Whereas one group had no hypothesis as to the identity of this AZT metabolite (29), the other group suggested that this unknown metabolite might represent AZT-nucleotides (30). However, specific hydrolysis by alkaline phosphatase or 5′-phosphodiesterase or chemical identification was not performed. In light of our data, which demonstrate AMT formation in liver cells, degradation of AZT to AMT may be found at different sites, thus opening to question whether this catabolic pathway has been underestimated in previous metabolic studies of AZT. Reexamination of AZT metabolism in human placenta would be particularly important, due to the potential toxicity that AMT may present to the developing fetus.

In view of the substantial intracellular and extracellular

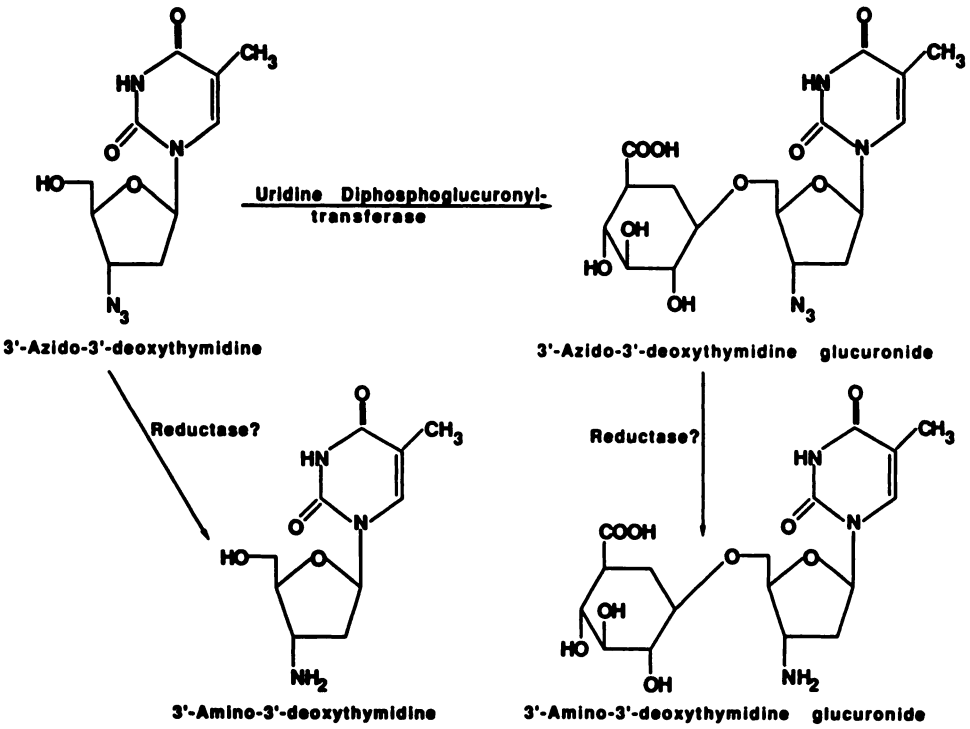

Fig. 7. Proposed catabolic pathway of AZT in liver cells.

levels of AMT detected following exposure of hepatocytes to 10 μM [^{3}H]AZT and the previous studies by Prusoff's group (13) on the inhibitory effect of AMT on DNA polymerase α, direct effects of AMT on myeloid and erythroid human progenitor cells *in vitro* were assessed. AMT was 5- to 7-fold more toxic to both CFU-GM and BFU-E than was AZT. Although AMT plasma levels have not yet been reported in patients after AZT administration, it appears from these *in vitro* tests that only 0.1 μM AMT and/or a 1:10 ratio of AMT to AZT in plasma might be sufficient for this AZT catabolite to exert myelosuppressive effects. Relevant to the present report, recent studies by our group in rhesus monkeys, an appropriate animal model for AZT disposition and metabolism (31, 32) have demonstrated the formation of both AMT and GAMT, in addition to GAZT, after administration of the parent drug, indicating that these catabolic pathways also occur *in vivo*.[1] In particular, AMT was present in plasma of each monkey at multiple time points between 30 min and 6 hr following subcutaneous administration of 33.3 mg/kg AZT. The AZT/AMT ratios ranged between 11.1 ± 1.7 and 2.7 ± 1.0, values measured at the C_{max} and C_{min} of both compounds, respectively. These data suggest that AMT formation at the hepatic site leads to sufficient AMT plasma levels *in vivo* that could contribute to the myelosuppressive effects of AZT. The mechanism(s) of AMT toxicity remains to be elucidated; however it may be explained in part either by a higher rate of phosphorylation in bone marrow cells, with increased AMT-5′-triphosphate levels, as compared with AZT, or more likely from a lower K_i value (3.3 μM) for DNA polymerase α (13), as compared with AZT, which has a K_i value of approximately 230 μM (33). These data thus suggest that AMT may play a role in the AZT-induced cytotoxicity to myeloid and erythroid cells in patients with acquired immunodeficiency syndrome. The third step in the catabolic pathway of AZT involves the reduction of GAZT to GAMT. Low levels of GAMT were detected within the cell, whereas none could be detected in the extracellular medium, possibly due to its low levels in the intracellular medium combined with a limited permeability due to its large carbohydrate moiety, as observed for GAZT. These data suggest that GAMT is probably a minor metabolite of AZT.

In summary, these findings demonstrate the rapid catabolic conversion of AZT to GAZT, AMT, and GAMT in liver cells. Initial studies have indicated that formation and excretion of GAZT in rats are minimal when compared with those in humans (2), consistent with demonstrated decreased efficiency of GAZT formation in rat as compared with human microsomes (9, 10). The data presented here demonstrate that GAZT is substantially formed in isolated rat hepatocytes. Although decreased formation of GAZT in rat cells as compared with human cells may be an important cause of the different metabolic ratios of GAZT/AZT detected in urine of these two species, it is also possible that, once formed in rat liver cells, GAZT may be excreted in bile (11, 28) and hydrolyzed to AZT by β-glucuronidase located in the small intestine (34). In addition, bacterial β-glucuronidase activity within the urinary tract is extremely high in rats (34), leading to a potential hydrolysis of GAZT to AZT at that site. In either case, GAZT levels excreted in the urine would be minimal, accounting for the minimal GAZT detected in urine of rats.

Of particular interest was the unexpected finding of two catabolites, AMT and GAMT, that were formed within hepatocytes. These metabolites were resolved from GAZT and did not coelute with any known AZT anabolites. A number of characteristics of the formation, disposition, and biological significance of these two metabolites were established. (i) AMT formation is NADPH dependent. (ii) Once formed within the hepatic intracellular milieu, AMT is slowly released into the

[1] E. M. Cretton, R. F. Schinazi, H. M. McClure, D. C. Anderson, and J. P. Sommadossi. Pharmacokinetics of 3′-azido-3′-deoxythymidine and its catabolites and interactions with probenecid in rhesus monkeys. Submitted for publication.

extracellular medium. Interestingly, as demonstrated by using intact hepatocytes and microsomal systems, AMT is not a substrate for UDPGT; thus, this metabolite is not further degraded, and formation of GAMT is only related to the reduction of GAZT. (iii) AMT is highly toxic to human hematopoietic cells *in vitro*.

This is the first report on the complete catabolic profile of AZT at the hepatic site, and data support the critical role of the liver as a major factor in the clearance of AZT from the systemic circulation. The formation of AMT and GAMT by human microsomal preparations further suggests that the formation of AMT and GAMT in humans is very likely and should be reexamined. These data demonstrate the need to quantitate the formation of these catabolites in patients, as well as to evaluate the importance of these novel catabolic pathways as a route of AZT elimination once glucuronidation has been saturated.

Acknowledgments

We would like to thank Mr. Marion Kirk, Southern Research Institute, for preparing the FAB mass spectral analysis, and Janna Stockinger, for preparing and editing this manuscript.

References

1. Sommadossi, J. P., R. Carlisle, and Z. Zhu. Cellular pharmacology of 3′-azido-3′-deoxythymidine, with evidence of incorporation into DNA of human bone marrow cells. *Mol. Pharmacol.* **36**:9–14 (1989).
2. Hao, Z., D. A. Cooney, N. R. Hartman, C. F. Perno, A. Fridland, A. L. DeVico, M. G. Sarngadharan, S. Broder, and D. G. Johns. Factors determining the activity of 2′,3′-dideoxynucleosides in suppressing human immunodeficiency virus *in vitro*. *Mol. Pharmacol.* **34**:431–435 (1988).
3. Frick, L. W., D. J. Nelson, M. H. St. Clair, P. A. Furman, and T. A. Krenitsky. Effects of 3′-azido-3′-deoxythymidine on the deoxynucleotide triphosphate pools of cultured human cells. *Biochem. Biophys. Res. Commun.* **154**:124–129 (1988).
4. Balzarini, J., P. Herdewijn, and E. De Clercq. Differential patterns of intracellular metabolism of 2′,3′-didehydro-2′,3′-dideoxythymidine and 3′-azido-2′,3′-dideoxythymidine, two potent anti-human immunodeficiency virus compounds. *J. Biol. Chem.* **264**:6127–6133 (1989).
5. Balzarini, J., R. Pauwels, M. Baba, P. Herdewijn, E. De Clercq, S. Broder, and D. G. Johns. The *in vitro* and *in vivo* anti-retrovirus activity, and intracellular metabolism of 3′-azido-2′,3′-dideoxythymidine and 2′,3′-dideoxycytidine are highly dependent on the cell species. *Biochem. Pharmacol.* **37**:897–903 (1988).
6. Blum, M. R., S. H. T. Liao, S. S. Good, and P. De Miranda. Pharmacokinetics and bioavailability of zidovudine in humans. *Am. J. Med.* **85**:189–194 (1988).
7. Good, S. S., C. S. Koble, R. Crouch, R. L. Johnson, J. L. Rideout, and P. De Miranda. Isolation and characterization of an ether glucuronide of zidovudine, a major metabolite in monkeys and humans. *Drug Metab. Dispos.* **18**:321–326 (1990).
8. Good, S. S., D. T. Durack, and P. De Miranda. Biotransformation in various species and in humans of 3′-azido-3′-deoxythymidine, a potential agent for treatment of AIDS. *Fed. Proc.* **45**:444 (1986).
9. Cretton, E. M., D. V. Waterhous, R. Bevan, and J.-P. Sommadossi. Glucuronidation of 3′-azido-3′-deoxythymidine by rat and human liver microsomes. *Drug Metab. Dispos.* **18**:369–372 (1990).
10. Resetar, A., and T. Spector. Glucuronidation of 3′-azido-3′-deoxythymidine: human and rat enzyme specificity. *Biochem. Pharmacol.* **38**:1389–1393 (1989).
11. Mays, D. C., A. Baldoa, L. J. Pawluk, S. Nawoot, G. Apseloff, and N. Gerger. The rat is a useful model for studying azidothymidine pharmacokinetics. *Clin. Pharmacol. Ther.* **47**:157 (1990).
12. Lin, T. S., P. H. Fischer, and W. H. Prusoff. Effect of 3′-amino-3′-deoxythymidine on L1210 and P388 leukemia in mice. *Biochem. Pharmacol.* **31**:125–128 (1982).
13. Chen, M. S., K. L. Woods, and W. H. Prusoff. Molecular basis of the antineoplastic activity of 3′-amino-3′-deoxythymidine. *Mol. Pharmacol.* **25**:441–445 (1984).
14. Hirsh, M. S. Azidothymidine. *J. Infect. Dis.* **157**:427–431 (1988).
15. Richman, D. D., M. A. Fischl, M. H. Grieco, M. S. Gottlieb, P. A. Volberding, O. L. Laskin, J. M. Leedom, J. E. Groopman, D. Mildvan, M. S. Hirsch, G. G. Jackson, D. T. Durack, S. Nusinoff-Lehrman, and AZT Collaborative Working Group. The toxicity of azidothymidine (AZT) in the treatment of patients with AIDS and AIDS-related complex: a double-blind, placebo-controlled trial. *N. Engl. J. Med.* **317**:192–197 (1987).
16. Surbone, A., R. Yarchoan, N. McAtee, M. R. Blum, M. Maha, J. Allain, R. V. Thomas, H. Mitsuya, S. N. Lehrman, H. Kessler, C. E. Myers, and S. Broder. Treatment of the acquired immunodeficiency syndrome (AIDS) and AIDS-related complex with a regimen of 3′-azido-3′-dideoxythymidine (azidothymidine or zidovudine) and Acyclovir. *Ann. Intern. Med.* **108**:534–540 (1988).
17. Lin, T. S., and W. H. Prusoff. Synthesis and biological activity of several amino analogues of thymidine. *J. Med. Chem.* **21**:109–112 (1978).
18. Berry, M. N., and D. S. Friend. High yield preparation of isolated rat liver parenchymal cells: a biochemical and fine structure study. *J. Cell Biol.* **43**:506–520 (1969).
19. Sommadossi, J.-P., D. A. Gewirtz, R. B. Diasio, B. Aubert, J.-P. Cano, and I. D. Goldman. Rapid catabolism of 5-fluorouracil in freshly isolated rat hepatocytes as analyzed by high performance liquid chromatography. *J. Biol. Chem.* **257**:8171–8176 (1982).
20. Cybulski, R. L., D. W. Fry, and I. D. Goldman. Adenosine stimulation of uphill adenine transport in L1210 leukemia cells. *J. Biol. Chem.* **256**:4455–4459 (1981).
21. Lowry, O. H., N. J. Rosebrough, A. L. Farr, and R. J. Randall. Protein measurements with the Folin phenol reagent. *J. Biol. Chem.* **193**:265–275 (1951).
22. Sommadossi, J.-P., and R. Carlisle. Toxicity of 3′-azido-3′-deoxythymidine and 9-(1,3-dihydroxy-2-propoxymethyl)guanine in normal human hematopoietic progenitor cells *in vitro*. *Antimicrob. Agents Chemother.* **31**:452–454 (1987).
23. Zimmerman, T. P., W. B. Mahony, and K. L. Prus. 3′-Azido-3′-deoxythymidine: an unusual nucleoside analogue that permeates the membrane of human erythrocytes and lymphocytes by nonfacilitated diffusion. *J. Biol. Chem.* **262**:5748–5754 (1987).
24. Schinazi, R. F., J.-P., Sommadossi, V. Saalmann, D. L. Cannon, M.-Y. Xie, G. C. Hart, G. A. Smith, and E. F. Hahn. Activities of 3′-azido-3′-deoxythymidine nucleotide dimers in primary lymphocytes infected with human immunodeficiency virus type I. *Antimicrob. Agents Chemother.* **34**:1061–1067 (1990).
25. Sommadossi, J.-P., Z. Zhu, R. Carlisle, M.-Y. Xie, D. A. Weidner, and M. H. el Kouni. Novel pharmacologic approaches for the treatment of AIDS and potential use of uridine phosphorylase inhibitors, in *Advances in Chemotherapy of AIDS* (R. B. Diasio and J. P. Sommadossi, eds.). Pergamon Press, Inc., New York, 63–73 (1990).
26. Handlon, A. L., and N. J. Oppenheimer. Thiol reduction of 3′-azidothymidine to 3′-aminothymidine: kinetics and biological implications. *Pharmacol. Res.* **5**:297–299 (1988).
27. Kamali, F., A. Gescher, and J. A. Slack. Medicinal azides. 3. The mechanism of investigational antitumor agent *meta*-azidopyrimethamine in mouse tissue *in vitro*. *Xenobiotica* **18**:1157–1164 (1988).
28. De Miranda, P., T. C. Burnette, and S. S. Good. Tissue distribution and metabolic disposition of zidovudine in rats. *Drug Metab. Dispos.* **18**:315–320 (1990).
29. Liebes, L., S. Mendoza, D. Wilson, and J. Dancis. Transfer of zidovudine (AZT) by human placenta. *J. Infect. Dis.* **161**:203–207 (1990).
30. Schenker, S., R. F. Johnson, T. S. King, R. S. Schenken, and G. I. Henderson. Azidothymidine (zidovudine) transport by the human placenta. *Am. J. Med. Sci.* **299**:16–20 (1990).
31. Boudinot, F. D., R. F. Schinazi, T. M. Gallo, H. M. McClure, D. C. Anderson, K. J. Doshi, P. C. Kambhampthi, and C. K. Chu. 3′-Azido-3′-deoxyuridine (AzddU): comparative pharmacokinetics with 3′-azido-3′-deoxythymidine (AZT) in monkeys. *AIDS Res. Hum. Retrovirus* **6**:219–228 (1990).
32. De Miranda, P. T., C. Burnett, and S. S. Good. Disposition and pharmacokinetics of the antiviral drug 3′-azido-3′-deoxythymidine (Retrovir) in monkeys and rats, in *Abstracts of the Twenty-Seventh Interscience Conference on Antimicrobial Agents and Chemotherapy* (American Society of Microbiology, eds.). American Society of Microbiology, New York, 372 (1987).
33. Furman, P. A., J. A. Fyfe, M. H. St. Clair, K. Weinhold, J. L. Rideout, G. A. Freeman, S. N. Lehrman, D. P. Bolognesi, S. Broder, H. Mitsuya, and D. W. Barry. Phosphorylation of 3′-azido-3′-deoxythymidine and selective interaction of the 5′-triphosphate with human immunodeficiency virus reverse transcriptase. *Proc. Natl. Acad. Sci. USA* **83**:8333–8337 (1986).
34. Levvy, G. A., and J. Conchie. β-Glucuronidase and the hydrolysis of glucuronides, in *Glucuronic Acid, Free and Combined*. (G. J. Dutton, ed.). Academic Press, Inc., New York, 301–357 (1966).

Send reprint requests to: Jean-Pierre Sommadossi, University of Alabama at Birmingham, Department of Pharmacology, University Station, P.O. Box 600, Birmingham, AL 35294.